JOURNAL OF Applied Polymer SCIENCE

Increasing the Elongation at Break of Polyhydroxybutyrate Biopolymer: Effect of Cellulose Nanowhiskers on Mechanical and Thermal Properties

Patrícia S. de O. Patrício,[1] Fabiano V. Pereira,[2] Meriane C. dos Santos,[1] Patterson P. de Souza,[1] Juan P. B. Roa,[3] Rodrigo L. Orefice[4]

[1]Centro Federal de Educação Tecnológica de Minas Gerais, Av. Amazonas, 5253, Belo Horizonte, MG CEP 30421-169, Brazil
[2]Departamento de Química, Universidade Federal de Minas Gerais, Av. Antônio Carlos, 6627, Pampulha, Belo Horizonte, MG CEP 31270-901, Brazil
[3] Instituto de Ciência e Tecnologia – Universidade Federal dos Vales do Jequitinhonha e Mucuri- Campus JK -Rodovia MGT 367/Km 583, 5000 - Alto da Jacuba- Diamantina/MG CEP- 39100-000.
[4]Departamento de Engenharia Metalúrgica e de Materiais, Universidade de Federal de Minas Gerais, Av. Antônio Carlos, 6627, Pampulha, Belo Horizonte, MG CEP 31270-901, Brazil
Correspondence to: P. S. de O. Patrício (E-mail: patriciapatricio@des.cefetmg.br)

ABSTRACT: Bionanocomposites based on polyhydroxybutyrate (PHB) and cellulose nanowhiskers (CNWs) were prepared by dispersing CNWs in poly(ethylene glycol) (PEG) plasticizer subsequently incorporating the CNWs/PEG suspensions in the matrix. The thermal properties of the nanocomposites indicate an enlargement in the processing window in comparison to the neat PHB. The nanocomposites showed a remarkable increase in the strain level (50 times related to the neat PHB), without a significant loss of the tensile strength with the incorporation of small concentrations of CNWs in the final nanocomposite (up to 0.45 wt %). This behavior was explained in terms of a considerable chain orientation promoted by the presence of CNWs in the same direction of the applied load, which activated shear flow of the polymer matrix. The results described here can be explored to extend the applications of this biopolymer. © 2012 Wiley Periodicals, Inc. J. Appl. Polym. Sci. 000: 000–000, 2012

KEYWORDS: biopolymers and renewable polymers; mechanical properties; nanoparticles; nanowires and nanocrystals

Received 18 March 2012; accepted 29 March 2012; published online 00 Month 2012
DOI: 10.1002/app.37811

INTRODUCTION

Motivated by the need to develop environmental friendly materials based on renewable natural resources, the polyhydroxyalkanoate (PHAs) family has been widely investigated. PHAs are biopolyesters synthesized by a wide variety of microorganisms and degraded by different bacteria, fungi, and algae in various ecosystems. Biologically produced, polyhydroxybutyrate (PHB) is a semicrystalline isotactic stereoregular polymer with 100% R configuration that allows a high level of degradability.[1] Besides its biodegradability, this polymer is also biocompatible, allowing its application in the biomedical field, especially in tissue engineering.[2,3] Currently, PHB applications range from surgical sutures, drug-delivery systems,[4] and agricultural foils to packaging for the storage of food products.[5]

In addition, isostatic PHB shows some properties comparable to petroleum-based polymers (e.g., polypropylene (PP)), such as high melting temperature (~ 175°C) and relatively high tensile strength (~ 30 MPa). However, PHB has had only limited use mainly because of its brittleness (presenting low strain at break) and the narrow processing window of this plastic. Indeed, the elongation at break is very different between PHB (~ 5%) and PP (~ 400%). Moreover, PHB thermally decomposes at temperatures just above its melting point.

Several methods have been developed to manage the disadvantages of PHB. One of the main approaches is the production of derivatives based on PHB via the biosynthesis of copolyesters containing PHB units with other 3-hydroxyalkanoates units,[6] such as poly(3-hydroxybutyrate-*co*-hydroxyvalerate) (PHBV)[7] or poly(3-hydroxybutyrate-*co*-3-hydroxyhexanoate),[8] with different

molar ratios of hydroxycarboxylic acids. This approach has been investigated extensively[9] because it can effectively improve mechanical properties[10] and lower the melting point, avoiding degradation during processing. However, blends and composites based on PHB that exclude any synthetic step are also very convenient as industrial materials due to their easy processability and lower cost.[11]

The addition of plasticizers is also considered a relatively simple route to modify the thermal and mechanical properties of polymers. Poly(ethylene glycol), PEG, is an organic solvent and nontoxic plasticizer that is biocompatible and soluble in water. Parra et al.[12] showed that, by increasing the concentrations of low molecular weight PEG in PHB/PEG blends (up to 40% of PEG), there was an increase in the elongation at break up to about four times the original elongation at break of PHB and a reduction in the tensile strength.

Finally, particles or fibers as reinforcing agents have been used to produce composites or nanocomposites based on PHB biopolymer as a way to improve its performance. Metal nanoparticles show catalytic, electrical, and sensing properties and may enhance the thermal stability of the PHB, as reported by Yeo et al.[13] Multiwalled carbon nanotubes (MWCNTs) and bioactive glass particles have been incorporated in the PHB matrix to enable tissue engineering applications.[14] The incorporation of bioactive glass particles and MWCNTs in PHB polymer has been carried out not only to act as reinforcing agents but also due to the specific properties of these particles. The introduction of bioactive glass particles has the advantage to enhance the bioactivity of the composite and the incorporation of MWCNTs leads to a conductive network that can act as a sensor to detect the bioactivity of PHB/bioactive glass composites. Regarding changing the mechanical properties with the addition of nanotubes, it was reported that, with lower contents of MWCNT (0.2–2 wt %), the Young's modulus and crystallinity increase linearly with nanotube volume fraction.[2,14,15] Other types of nanoreinforcements introduced into the PHB matrix were clays, such as organophilic montmorillonite.[16] The incorporation of the organophilic Cloisite 25A improved the thermal stability of PHB.[17]

Cellulose nanowhiskers (CNWs), also called cellulose nanocrystals, are highly crystalline rod-like nanostructures obtained from cellulose.[18] They can be obtained through a controlled acid hydrolysis from a large variety of natural cellulose sources, including reforestation wood or agricultural residue.[19] The acid hydrolysis readily destroys the amorphous regions of the cellulose, leaving the crystalline segments intact and leading to the formation of high-purity single crystals. The average CNWs dimensions are 100–250 nm in length and 5–15 nm in diameter for acid-hydrolyzed nanowhiskers obtained from a majority of cellulose fibers.[20] Besides their high aspect ratio, the advantages of using CNWs for the design of new bio-based nanocomposites include their renewability, low density, and high specific mechanical properties.[21] The Young's modulus of CNWs is close to that of the perfect crystal[22] of native cellulose (around 100 GPa), similar to that of steel or Kevlar. The strength of the nanowhiskers is in the order of 10 GPa.[22]

Recently, a nanocomposite prepared using PHBV with the addition of freeze-dried CNWs (2 and 5 wt %) containing PEG was investigated by Ten et al.[23] The influence of CNW powder on the mechanical, physical, and chemical properties of PHBV matrix was investigated. The results indicate that the use of CNW increased the tensile strength of the polymer. However, the authors reported a lower elongation at break with the addition of nanowhiskers in the studied concentration range.

In this work, a bionanocomposite based on the homopolymer PHB with PEG and with different low concentrations of CNW (between 0 and 0.75 wt %) was produced by the solvent casting method using chloroform as solvent. PEG was used to increase the compatibility between CNW and PHB, and its content related to the polymer amount was kept constant (15 wt %). The morphology, thermal stability, and mechanical properties of the bionanocomposites were investigated.

EXPERIMENTAL

Materials

PHB powder was supplied by PHB Industrial (Serrana, SP, Brazil) registered under the brand BIOCYCLE®. Chloroform and PEG (average molecular weight of 200 g mol^{-1}) were obtained from Sigma-Aldrich.

CNWs Preparation. Sulfuric acid hydrolysis of eucalyptus wood pulp was performed as described in the literature and in our previous work with minor modifications.[24,25] Briefly, the wood pulp was ground until a fine particulate was obtained using a Willey mill. Then, 10.0 g of cellulose was added to 80.0 mL of 64 wt % sulfuric acid under strong mechanical stirring. Hydrolysis was performed at 50°C for about 50 min. After hydrolysis, the dispersion was diluted twofold in water, and the suspensions were then washed using three repeated centrifuge cycles. The last washing was conducted using dialysis against deionized water until the dispersion reached pH $\sim$ 6.0. Afterward, the dispersions were ultrasonicated with a Cole Parmer Sonifier cell disruptor equipped with a microtip for 8 min and finally filtered using a 20-μm pore size filter.

Sample Preparation

Samples were prepared by the solvent casting method. PHB was solubilized in chloroform (5%, w/v) at 40°C through constant stirring until complete dissolution of the polymer. CNWs were completely dispersed in PEG by solvent exchange through the evaporation of water to obtain the desired concentrations of nanowhiskers in PEG of 0.0; 0.15; 0.3; 0.5; 1.0; 1.5; 3.0; and 5.0 wt %. The as-prepared dispersions of CNWs in PEG were added to the PHB polymer (solution in chloroform), keeping the amount of PEG in PHB constant and equal to 15 wt % for all the samples. When necessary, PEG (without CNWs) was added to the samples to have the final concentration (in wt %) of PEG related to the weight of PHB polymer equal to 15 wt %. The dispersions were stirred for 24 h to prepare the following final concentrations of nanowhiskers in the nanocomposites: 0.0; 0.022; 0.045; 0.075; 0.15; 0.22; 0.45; and 0.75 wt %. The samples were cast on Petri dishes, which were left at room temperature until the solvent was evaporated to yield free-standing films. The residual solvent was further removed at 40°C for 3 days.

Methods

The morphological study of PHB plasticized with PEG (PHB/PEG) and PHB/PEG/CNW nanocomposites was carried out with a JEOL instrument, model 840A, scanning electron microscope (SEM) operating at 15 kV. The samples were immersed in liquid nitrogen and were broken. The fractured surfaces were coated with a 2 nm layer of gold using a BAL-TEC MC5 010 automated sputter coater.

Transmission electron microscopy (TEM) images of the nanocomposites were taken using a FEI Tecnai G2-Spirit with a 120 kV acceleration voltage. The microtomed surfaces of the nanocomposites were prepared by cutting small pieces with a diamond knife in a Leica EM UC6 ultramicrotome, generating foils with a thickness of 50 nm. The samples were deposited on a carbon-formvar-coated copper (300 mesh) TEM grids.

Fourier transform infrared (FTIR) measurements were carried out with Nicolet 320 spectrophotometer with a horizontal attenuated reflection (ATR) accessory. The spectra of the samples were obtained in the region from 4000 to 600 cm^{-1} using a ZnSe crystal.

The thermal degradation profile was measured for the PHB/PEG and PHB/PEG/CNW nanocomposite by using a Shimadzu instruments model thermogravimetric analysis (TGA) 60 H by increasing the temperature from 25 to 600°C at a heating rate of 20°C min^{-1}. The weight of each sample was typically 4–10 mg when placed in an alumina pan. The samples were heated under air.

Uniaxial tensile mechanical testing to evaluate the mechanical properties of the materials was performed using a universal testing machine EMIC model DL 3000 with a 200 *N* load cell and a speed of 25 mm min^{-1}. The samples were obtained by pressing the films against a ASTM D638 die at 170°C and using 200 Kg/cm^2 of pressure. Mechanical tensile data were averaged over at least 10 specimens, and the results had good reproducibility in all cases.

RESULTS AND DISCUSSION

Morphological Properties

The size characterization (using TEM) of the eucalyptus CNWs used in this work was already described in two of our previous papers.[19,25] The mean values of the length and diameter of the isolated nanowhiskers were determined to be 145 ± 25 nm and 6.0 ± 1.5 nm, respectively.

On the preparation of nanocomposites using CNWs, one of the major challenges is the appropriate compatibilization of the nanoreinforcements with the polymer to achieve an acceptable dispersion level of the filler within the polymeric matrix. In this work, the CNWs were dispersed in the PHB matrix using low molar mass PEG as the dispersing agent. Because of the strong hydrogen bonds established between the CNWs and PEG, it was possible to disperse them in this plasticizer. Figure 1 shows flow birefringence found in the PEG/CNWs suspensions at 1 wt % concentration, as observed between two crossed polarizers. The appearance of flow birefringence, which results from the induced alignment of the rod-like nanoparticles under flow, indicates the presence of isolated CNWs in the suspension.

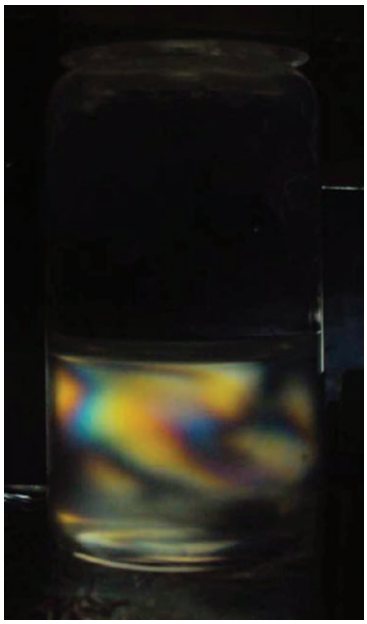

Figure 1. PEG/CNWs dispersion at 1 wt % concentration, observed between crossed polarizers.[Color figure can be viewed in the online issue, which is available at wileyonlinelibrary.com.]

It is important to mention that, even though the presence of the plasticizer (PEG) is essential to appropriately disperse the CNWs within the matrix, we tried to prepare the same nanocomposites without PEG. As expected, it was not possible to disperse the CNWs in the solvent casting nanocomposites. The flocculation of the nanowhiskers in chloroform was strong and during the preparation of the composite (by mixing the CNWs and polymer solution in the same solvent), a total phase separation and precipitation of the nanowhiskers took place and the preparation of the composites without PEG was not possible.

The morphology of the fracture surface of the PHB/PEG materials with and without the presence of whiskers was investigated by SEM. For the PHB/PEG system (without CNWs), the SEM image [Figure 2(a)] revealed a fracture morphology typical of a brittle material, with the crack propagation developing preferably along a unique direction (highlight with arrows). On the other hand, the PHB/PEG/CNW nanocomposite with 0.075 wt % of CNWs, Figure 2(b), showed a modification in the morphology of the fracture mode when compared with the PHB/PEG system. Figure 2(c) shows the SEM image for the same nanocomposite (with 0.075 wt %) in a higher magnification. The fractures surfaces showed by the nanocomposite with 0.075 wt % of CNWs have different features compared to the sample without CNWs and can be associated with a much more ductile failure. The formation of lamellas and the presence of a preferential direction in the fracture were not observed when the CNWs were present in the composites. More important, SEM images of the PHB/PEG/CNW nanocomposites did not show the presence of large agglomeration of the CNWs, for all magnitudes investigated. It is a first indication that CNWs could be well dispersed in the matrix.

Applied Polymer SCIENCE

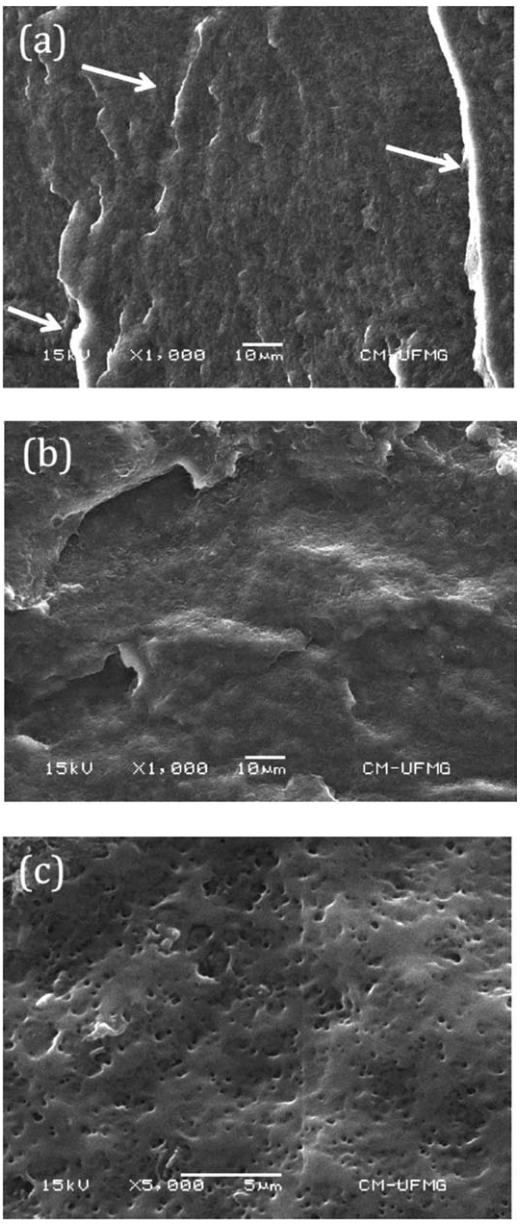

Figure 2. SEM images of the cryofracture surfaces of the nanocomposites PHB/PEG/CNW with 0 wt % (a) and 0.075 wt % at ×1000 magnification (b), and 0.075 wt % at ×5000 magnification (c).

To appropriately characterize the dispersion of the nanowhiskers within the matrix, the PEG/CNW/PHB bionanocomposites were also studied using TEM. Figure 3 shows a typical TEM image obtained from a microtomed surface of the PEG/CNW/PHB sample with 0.15 wt % of CNWs. The CNWs were essentially dispersed in the PHB matrix and did not present large agglomerates. In conclusion, for this system, the dispersion of the CNWs in the polymeric matrix seemed to be relatively efficient, possibly due to the presence of PEG, which can act as a coupling agent between the PHB and the nanowhiskers. The existence of interactions involving the components of this system was also investigated by FTIR-ATR and will be discussed in the next section.

Structure Properties

Since the addition of PEG molecules has the goal to completely disperse the nanowhiskers within the matrix and to increase the interfacial adhesion between the nanowhiskers and the polymer, we believe that the parameter that describes whether the nanowhiskers are completely covered by PEG or not is important to describe the nanocomposites. From the TEM data of CNWs size (145 nm in length and 6 nm in width), we could calculate the surface area of a single nanowhiskers as being 2790 nm^2. Given this high surface area of the nanowhiskers, it is highly expected that it is necessary an abundance of PEG (in wt %) with respect to the CNW to completely cover the surface of these nanowhiskers with low molecular weight PEG 200.

Figure 4 shows the ART-FTIR spectra of the PHB film plasticized with PEG (0 wt%) and those of the PHB/PEG/CNW nanocomposite films. Numbers labeling each spectrum indicate the amount of CNWs for each sample. The IR stretching bands of characteristic groups of PHB were predominant in spectra of all compositions due to the high concentration of the polymer in materials. The bands at 3000–2900 cm^{-1} are associated with the CH_3, CH_2 asymmetric, and CH_2 symmetric stretching vibrations. The deformation modes of vibration of these groups were observed at 1460–1350 cm^{-1}. Spectra of pure PHB and nanocomposites showed multiple bands in the 1300–1100 cm^{-1} region due to the stretching of C—O—C groups in the crystalline (1276 and 1226 cm^{-1}) and amorphous phases (1261 and 1183 cm^{-1}).

The stretching vibrations due to carbonyl are observed within the range of 1700–1650 cm^{-1}. This IR absorption band is an important spectral region to analyze in the case of PHB materials, because it is possible to assign crystalline and amorphous

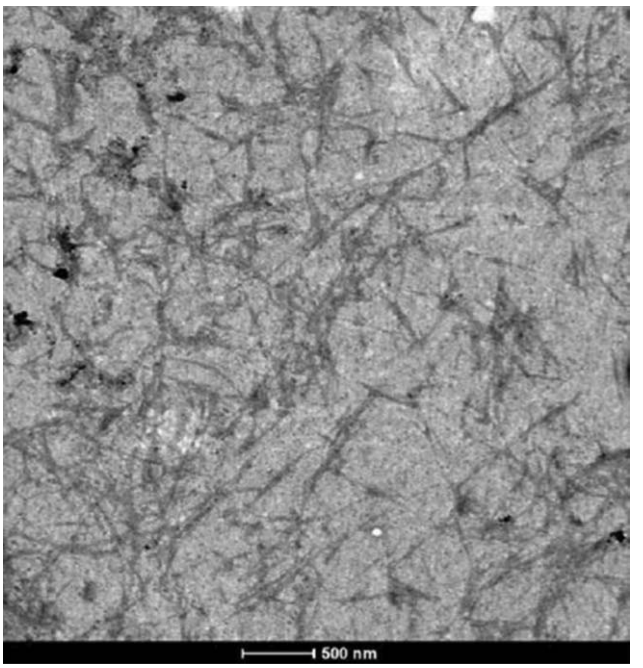

Figure 3. TEM image of the PHB/PEG/CNW nanocomposite with 0.15 wt % CNWs.

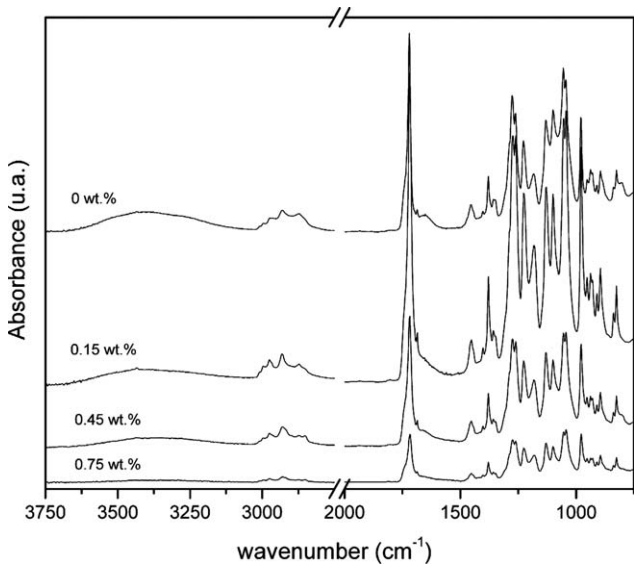

Figure 4. ATR-FTIR spectra of PHB/PEG/CNW nanocomposites (0.15, 0.45, and 0.75 wt %) and PHB/PEG system.

phases to 1720 and 1742 cm^{-1}, respectively.[26] In the case of composites or blends with PHB, the carbonyl region can exhibit three bands. Beyond the already two mentioned, the other one appears at 1709 cm^{-1} and can be attributed to C=O groups involved in hydrogen bonds.[27] Figure 5 shows the carbonyl region of PHB/PEG system and 0.15, 0.45, and 0.75 wt % nanocomposites. The signal curves were fitted using Gaussian functions. All the spectra showed the three contributions: crystalline, amorphous phase, and hydrogen bonded carbonyl groups.

The PHB/PEG/CNW normalized spectra showed broader bands at approximately 1710 cm^{-1} when compared with the PHB/PEG matrix spectrum. This behavior can be due to the hydrogen interactions between the C=O groups in PHB and OH groups in CNWs, which are different than those observed between the PHB and PEG groups. The interactions probably involve the groups present in amorphous phases.

The maximum absorbance values located at 1742 and 1720 cm^{-1} did not change their position according to Figure 5. These groups are less influenced by the formation of different interactions such as hydrogen bonds. However, the absorbance peak at 1710 cm^{-1} shifts to 1700 cm^{-1} for the nanocomposite with 0.75 wt % whiskers. It is an indication of the appearance of a different interaction for the nanocomposite with 0.75 wt % whiskers.

This result can be associated with the relative number of PEG molecules necessary to cover the surface of cellulose whiskers. If the concentration of PEG related to the PHB remained constant (15 wt % for all the nanocomposites), the PEG/CNW ratio decreased with the incorporation of CNW. As the CNWs have a high surface area, a small increase in the concentration of CNWs in the composites cause a significant increase in surface area to be covered. From the results obtained by FTIR, two situations can be proposed in relation to the ratio of total CNWs surface area/number of PEG molecules:

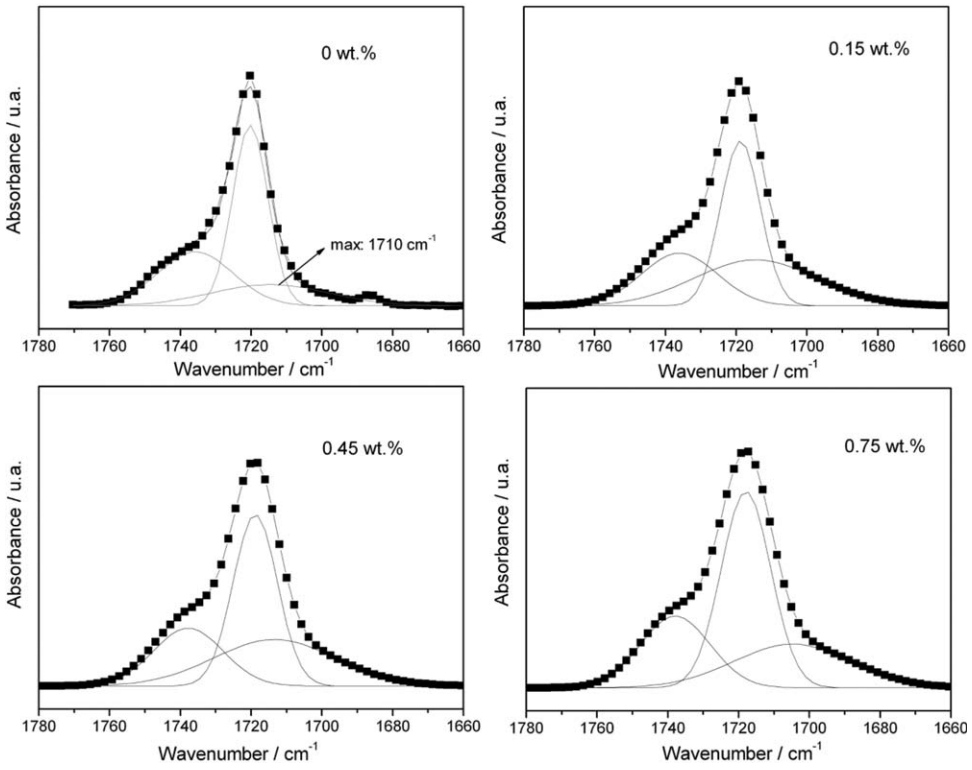

Figure 5. Fitted Gaussian FTIR-ATR curves for PHB/PEG and the nanocomposites (whiskers concentrations are indicated in the plot). The guidelines show the shift of the absorbance band around 1700 cm^{-1}.

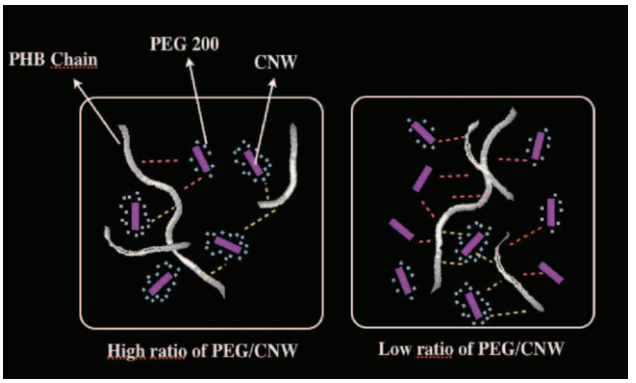

Scheme 1. Schematic representation of the types of interactions in the nanocomposites. [Color figure can be viewed in the online issue, which is available at wileyonlinelibrary.com.]

i. Low: it suggests that the CNWs are covered with PEG, forming hydrogen bonds between the C=O polar groups of PHB and OH groups of PEG. The direct interaction between CNWs (without PEG covering the nanowhiskers) and PHB is minor or even nonexistent in this case.
ii. High: PEG becomes relatively less available (as in the case of 0.75 wt % whiskers). In this way, the CNWs become more available to interact directly with the PHB matrix because the PEG concentration decreases in relation to CNW.

Scheme 1 summarizes the hypotheses described above and suggests a kind of critical concentration in the range of 0.45–0.75 wt% CNWs in the PHB/PEG systems based on the micelle theory. The idea of CNWs covered by PEG was already suggested by Oksman et al.[21] in CNW/polylactic acid (PLA) nanocomposites studies.

Thermogravimetric Analysis

The thermal stability of the materials was investigated by thermogravimetric analysis, and the effect of the concentration of CNW on the thermal properties of the nanocomposites was also studied. TGA data obtained for the neat PHB, PHB/PEG matrix, and the PHB/PEG/CNW nanocomposites containing 0; 0.15; 0.45; and 0.75 wt % CNW are shown in Figure 6 and Table I. The TGA curve of the PHB/PEG matrix presents a two-stage weight loss. The first one at 228°C with 15 wt % of loss can be associated with the degradation of the PEG groups and the other at 287°C is related to the PHB groups. The incorporation of the CNWs nanoparticles increased the decomposition temperature of the polymeric matrix significantly in all stages of degradation, being more pronounced in the second stage, as shown in Figure 6. The observed shift in the weight loss was possibly due to reductions in both the thermal conductivity and diffusivity. TGA data obtained from freeze-dried CNWs (not shown here) showed the first weight loss at 278°C and the second one at 388°C. Based on the hypotheses that the CNWs were covered by PEG, it can be suggested that PEG becomes constricted in the nanocomposite, restricting structural degradation at higher temperatures. The increase in the decomposition temperature was more pronounced near to 0.45 wt % concentration (inset in Figure 6), because the interface between the

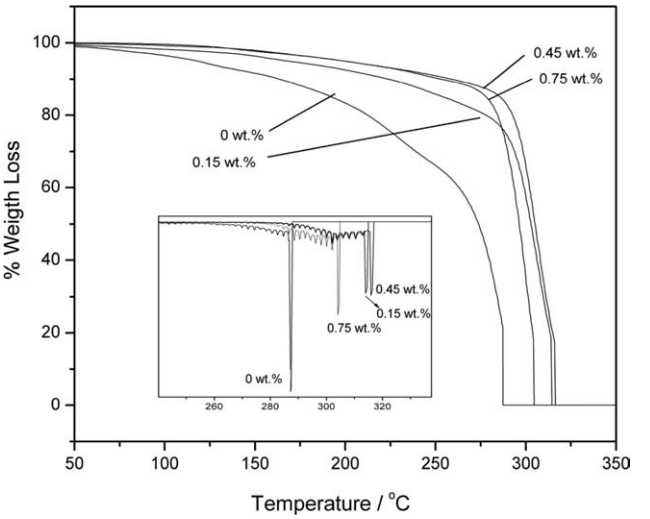

Figure 6. TGA and DTG (inset) curves of PHB/PEG and the nanocomposites. The CNWs concentrations are given in the figures.

CNWs covered with PEG and the PHB matrix is stronger when compared with the free CNWs (not covered by PEG) and the matrix. In this way, the degradation temperature of the 0.75 wt % sample decreases when compared with other nanocomposites because there is a higher concentration of CNWs without PEG.

Differential scanning calorimetry measurements (Table I) showed a decrease in the melting temperature of the nanocomposites compared to the neat PHB (from 175 to about 160°C). These results together with the increase in the decomposition temperature indicate an enlargement of the processing window of the nanocomposites compared to the neat PHB.

Mechanical Properties

The stress–strain curves for the PHB/PEG and the PHB/PEG/CNW nanocomposites are given in Figure 7. First, compared to the neat PHB film (not shown here), the incorporation of PEG leaded to a reduction in both the tensile strength (30–22 MPa) and the Young's modulus (1180–537 MPa), and it leaded to an increase in the elongation at break (from 6 to 12%). PHB is stiff and brittle, whereas PHB/PEG is softer and tougher, because PEG can allow chain flow with lower mechanical loads.[12] This result is highly expected and shows that PEG acts as plasticizer for PHB. It is important to mention at this point that the amount of PEG used for the PHB/PEG (0 wt % CNWs) is the same used for the others systems (15 wt % of PEG in all

Table I. Thermal Properties for the Neat PHB, PHB/PEG, and PHB/PEG/CNW Nanocomposites

Materials	T_m (°C)	T_{onset} (°C)	T_{max} (°C)
PHB	175	270	287
PHB/PEG	156	228	287
PHB/PEG/CNW 0.15%	160	272	314
PHB/PEG/CNW 0.45%	162	243	316
PHB/PEG/CNW 0.75%	163	276	304

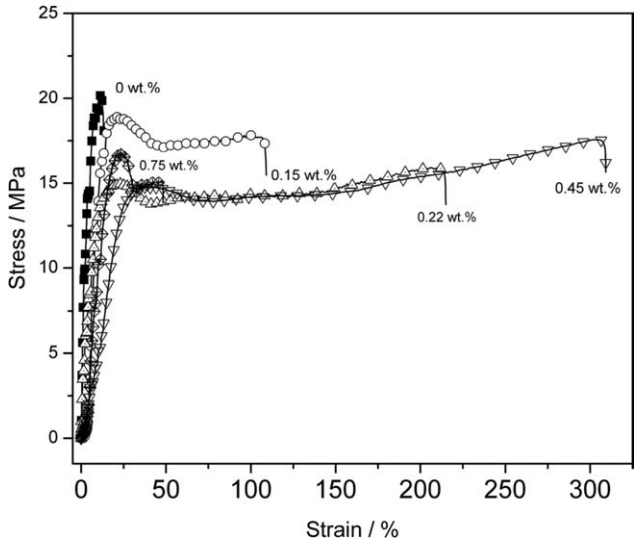

Figure 7. Stress–strain curves for the PHB/PEG (0 wt %) and PHB/PEG/CNW nanocomposites in different concentrations.

systems, related to the PHB polymer), as explained in Experimental section.

The tensile strengths of the PHB/PEG/CNW nanocomposites were reduced (by about 3.0 MPa) when compared with the PHB/PEG matrix without CNWs. An almost constant strength of 17 MPa was observed for all nanocomposites. In fact, the CNWs covered by PEG did not act as a reinforcing agent by PHB. The Young's modulus decreased remarkably with the incorporation of CNWs up to 0.45 wt % CNWs (Figure 8). After this concentration, an increase of the Young's modulus was observed due to the presence of CNWs not covered by PEG, which offer more resistance to the chain flow.

More importantly, the elongation at break of the bionanocomposites increased remarkably with the addition of CNWs containing PEG, as shown in Figure 7. The strain increased almost linearly with whisker concentrations up to 0.45 wt % (Figures 7 and 8), reaching a value of elongation at break about 25 times greater than that of the PEG/PHB sample. Other authors reported increase in the elongation at break with the incorporation of PEG/CNW in other biodegradable matrices such as cellulose acetate butyrate[28] and PLA.[21] However, in this work, a much greater change in the strain than those observed for butyrate[28] and PLA[21] was achieved with the addition of very low concentrations of nanowhiskers (from 0.022 to 0.45 wt %).

It is worth to mention that PHB/PEG/CNWs nanocomposites have also been prepared with higher concentrations of CNWs (1–5 wt %) and the same concentration of PEG. For the nanocomposites prepared in higher concentrations of CNW's no increase in the elongation was detected, while an increase in the tensile strength was detected, similarly described by other authors whom study PHBV matrices with CNW's using higher concentrations of nanowhiskers as the present study.[23]

To explain the significant increase in the elongation observed for the nanocomposites using low concentration of CNWs, the surface and fracture morphology of the films after break (tensile tests) were studied using SEM images. Figure 9 shows images of the surface of a PHB/PEG film [Figure 9(a,b)] and of a PHB/PEG/CNW film with 0.45 wt % nanowhiskers [Figure 9(c,d)] in different magnifications. The presence of cracks on the surface of PHB/PEG [Figure 9(b)], characteristic of a brittle matrix was observed. However, for the film with the CNW covered whit PEG, no cracks were observed and a remarkable orientation throughout the surface of the film in the same direction of the applied load could be seen [Figure 9(c,d)]. This orientation was observed not only on the films surface but also in the polymer bulk (observed through SEM study of cryo-fractures of the films, not shown here).

We can explain this remarkable behavior because PEG molecules strongly interact with the CNW and also with the PHB chains acting as an appropriate interface between the nanowhiskers and the polymer. Bundles of laterally aggregated CNW covered with PEG achieve sufficient mobility to orient together with the plasticized PHB parallel to the applied load [Figure 9(c,d)]. In this way, the slippage of individual and/or bundles of laterally aggregated CNWs and the molecular alignment during the plastic deformation can extensively activate shear flow of the polymer matrix allowing the system to sustain higher deformations without catastrophic fracture (evidenced by the process of strain hardening after the yield strength).

This behavior of slippages of oriented nanofibers with strong interfacial adhesion to the polymer matrix was already described by Kim et al.[29] In this work, the authors related a transformation of the deformation process from brittle to ductile in a polycarbonate with 4 wt % MWCNTs nanocomposite prepared by an electrospinning process. The authors stated that the applied stress could also be transferred to the orientated MWCNTs and, as a consequence of the slippage of the individual MWCNTs, and the oriented polymer molecules the shear flow of the polymer was activated.

In the nanocomposite with a concentration of CNWs = 0.75 wt %, a decrease in the elongation at break (to about 38% of the strain) was observed. This result can be attributed to the increase in concentration of CNWs without PEG and explained by the

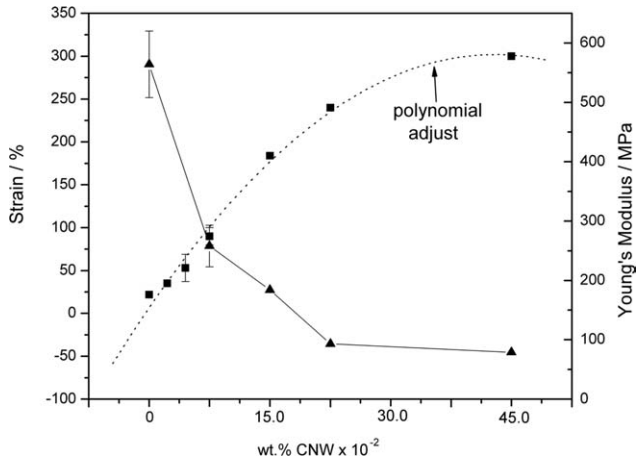

Figure 8. Elongation at break and Young's modulus as a function of CNW concentration in the bionanocomposites.

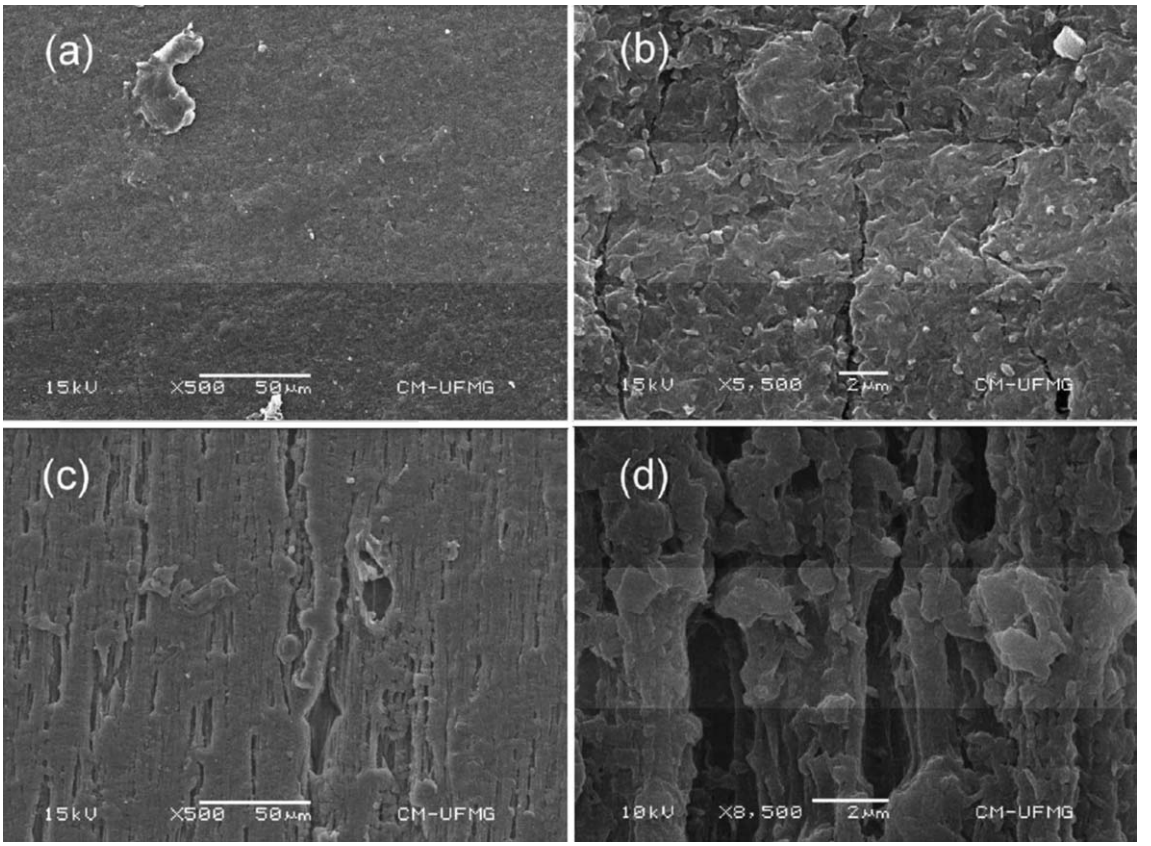

Figure 9. Surface film morphology of the PHB/PEG at ×500 (a) and ×5500 (b) and PHB/PEG/CNW with 0.45 wt % CNWs at ×500 (c) and ×8500 (d). Images obtained by SEM microscopy after tensile tests of the films.

poor interface between the phases. In fact, the angular coefficient of the curve in Figure 8 decreases after 0.22 wt %, demonstrating that a different effect begins to interfere, which is associated with the decrease of the PEG/CNW ratio. In addition, these results are in agreement with the FTIR results, which showed a different interaction in the nanocomposite with 0.75 wt % whiskers.

CONCLUSIONS

PHB/PEG/CNW nanocomposites with the same concentrations of PEG in all systems and different low concentrations of nanowhiskers were studied and showed structural, thermal, and mechanical properties that are interesting for both scientific and applied fields. Bionanocomposites based on PHB were prepared through the previous dispersion of CNWs in PEG plasticizer and subsequent incorporation of the PEG/ nanowhiskers dispersions into the biopolymer.

TEM image obtained from microtomed surfaces of the nanocomposites showed a good dispersion level of the CNWs in the matrix. Thermal properties studies revealed that the nanocomposites presented a larger processing window than the neat PHB because the maximum degradation temperature attributed to PHB was shifted to a greater temperature, whereas the melting temperature of the nanocomposites decreased compared to that of neat PHB.

The results presented here allowed the proposition of a model based on different possible interactions between the PHB, PEG, and CNW. When the ratio of PEG/CNW is high (for CNW concentrations up to 0.45 wt %), the CNWs are covered by PEG, and the interaction between the PHB and the CNWs occurs preferentially with PEG. In contrast, when the ratio PEG/CNW is low (CNW concentrations greater than 0.75 wt %), the interaction between PEG and PHB decrease, and the CNWs interact with the PHB matrix.

For concentrations of CNWs up to 0.45 wt %, a remarkable increase in the strain level was observed without a significant loss of strength. In this case, the elongation at break was improved by a factor of about 50 in relation to the neat PHB and by a factor of 25 in comparison to the PHB plasticized with PEG. The presence of the CNWs promoted a considerable chain orientation in the same direction of the applied load and greatly enhanced the elongation at break of the polymer through the slippage of the nanowhiskers and the oriented molecules during the plastic deformation. However, for the nanocomposite with a high concentration of CNWs (0.75 wt %), a decrease in the elongation at break and an increase of modulus were observed compared to the others nanocomposites. This result was explained in terms of the poor interface between the phases when the CNWs are not covered by PEG.

Given the interesting thermal and mainly the mechanical properties obtained here for the nanocomposites based on PHB biopolymer, this approach can potentially be explored as a strategy to extend the possible applications of this biopolymer. A similar system based on PHB/CNWs prepared from melting processes is under investigation and will be reported in a later work.

ACKNOWLEDGMENTS

The authors thank CNPq (CT- Ação Transversal/EDT N° 62/2008), CAPES (Nanobiotec - EDT N° 04/2008) and FAPEMIG (PPP- EDT N° 021/2008) for financial support. Centro de Microscopia-UFMG is also gratefully acknowledged for the TEM and SEM images.

REFERENCES

1. Noda, I.; Marchessault, R. H.; Terada, M. Polymer Data Handbook, Oxford University Press: London, **1999.**
2. Misra, S. K.; Ansari, T. I.; Valappil, S. P.; Mohn, D.; Philip, S. E.; Stark, W. J.; Roy, I.; Knowles, J. C.; Salih, V.; Boccaccini, A. R. *Biomaterials* **2010,** *31*, 2806.
3. Chen, G. Q.; Wu, Q. *Biomaterials* **2005,** *26*, 6565.
4. Errico, C.; Bartoli, C.; Chiellini, F.; Chiellini, E. *J. Biomed. Biotechnol.* **2009,** *2009*, 1.
5. Bucci, D. Z.; Tavares, L. B. B; Sell, I. *Polym. Test.* **2005,** *24*, 564.
6. Zhang, L.; Deng, X.; Zhao, S.; Huang, Z. *Polymer* **1997,** *38*, 6001.
7. Ahmed, T.; Marcal, H.; Lawless, M.; Wanandy, N. S.; Chiu, A; Foster, L. J. *Biomacromolecules* **2010,** *11*, 2707.
8. Qiu, Y. Z.; Han, J.; Guo, J. J.; Chen, G. Q. *Biotechnol. Lett.* **2005,** *27*, 1381.
9. Caballero, K. P.; Karel, S. F.; Register, R. A. *Int. J. Biol. Macromol.* **1995,** *17*, 86.
10. Zhao, K.; Deng, Y.; Chen, J. C.; Chen, G. Q. *Biomaterials* **2003,** *24*, 1041.
11. Avella, M.; Martuscelli, E.; Raimo, M. *J. Mater. Sci.* **2000,** *35*, 523.
12. Parra, D. F.; Fusaro, J.; Gaboardi, F.; Rosa, D. S. *Polym. Degrad. Stab.* **2006,** *91*, 1954.
13. Yeo, S. Y.; Tan, W. L.; Abu Baku, M.; Ismail, J. *Polym. Degrad. Stab.* **2010,** *95*, 1299.
14. Misra, S. K.; Ohashi, F.; Valappil, S. P.; Knowles, J. C.; Roy, I.; Silva, S. R.; Salih, V.; Boccaccini, A. R. *Acta Biomater.* **2010,** *6*, 735.
15. Coleman, J. N.; Cadek M.; Ryan, K. P.; Fonseca, A.; Nagy, J. B.; Blau, W. J.; Ferreira, M. S. *Polymer* **2006,** *47*, 8556.
16. Botana, A.; Mollo, M.; Eisenberg, P.; Sanchez, R. M. T. *Appl. Clay Sci.* **2010,** *47*, 263.
17. Erceg, M.; Kovacic, T.; Perinovic, S. *Thermochim. Acta* **2008,** *476*, 44.
18. Eichhorn, S. J.; Dufresne, A.; Aranguren, M.; Marcovich, N. E.; Capadona, J. R.; Rowan, S. J.; Weder, C.; Thielemans, W.; Roman, M.; Renneckar, S.; Gindl, W.; Veige, S.; Keckes, J.; Yano, H.; Abe, K.; Nogi, M.; Nakagaito, A. N.; Mangalam, A.; Simonsen, J.; Benight, A. S.; Bismarck, A.; Berglund, L. A.; Peijs, T. *J. Mater. Sci.* **2010,** *45*, 1.
19. de Mesquita, J. P.; Donnici, C. L.; Pereira, F. V. *Biomacromolecules* **2010,** *11*, 473.
20. Azizi Samir, M. A.; Alloin, F.; Dufresne, A. *Biomacromolecules* **2005,** *6*, 612.
21. Oksman, K.; Mathew, A. P.; Bondeson, D.; Kvien, I. *Compos. Sci. Technol.* **2006,** *66*, 2776.
22. Klemm, D.; Kramer, F.; Moritz, S.; Lindstrom, T.; Ankerfors, M.; Gray, D.; Dorris, A. *Angew. Chem. Int. Ed. Engl.* **2011,** *50*, 5438.
23. Ten, E.; Turtle, J.; Bahr, D.; Jiang, L.; Wolcott, M. *Polymer* **2010,** *51*, 2652.
24. Beck-Candanedo, S.; Roman, M.; Gray, D. G. *Biomacromolecules* **2005,** *6*, 1048.
25. de Mesquita, J. P.; Patricio, P. S.; Donnici, C. L.; Petri, D.; Oliveira, L. C. A.; Pereira, F. V. *Soft Matter* **2011,** *7*, 4405.
26. Furukawa, T.; Sato, H.; Murakami, R.; Zhang, J. M.; Duan, Y. X.; Noda, I.; Ochiai, S.; Ozaki, Y. *Macromolecules* **2005,** *38*, 6445.
27. Iriondo, P.; Iruin, J. J.; FernandezBerridi, M. J. *Macromolecules* **1996,** *29*, 5605.
28. Petersson, L.; Kvien, I.; Oksman, K. *Compos. Sci. Technol.* **2007,** *67*, 2535.
29. Kim, G. M.; Lach, R.; Michler, G. H.; Potschke, P. P.; Albrecht, K. *Nanotechnology* **2006,** *17*, 963.